(Fuji Film) and Image Quant Software (Molecular Dynamics, Sunnyvale, CA, USA).

Blood cytokine analysis

The blood pro-inflammatory cytokine concentration–related TLR4 signalling was determined as follows. The blood concentrations of IL-1α, IL-1β, IL-17, IFNγ and adiponectin were determined using a Milliplex®MAP Rat Cytokine/Chemokine/Adipocyte Immunoassay kit (Millipore Co. Billerica, MA, USA) or Luminex 100 KT01 (Luminex Co. Austin, TX, USA) in accordance with the manufacturers' instructions. Blood IFNα concentration was determined using an enzyme-linked immunosorbent assay kit (Uscn Life Science Inc. Wuhan, China).

Glutathione peroxidase assay

The activity of glutathione peroxidase (GPx), as an index of oxidative stress, in the liver was evaluated using the spectrophotometric method. A BIOTECH® GPx-340™ assay kit (Oxis Research ™ Burlingame, CA, USA) was used in accordance with the manufacturer's instructions.

Statistical analysis

Data are expressed as means ± SEM. Data were compared between the control and alcohol groups using the Fisher's exact test or the unpaired *t*-test with Welch's correction. A *P*-value of <0.05 was considered statistically significant. All statistical analysis was performed using GRAPHPAD PRISM 5.0c software for Mac OS X (GraphPad Software, Inc., La Jolla, CA, USA).

Results

Rats were fed with a liquid diet for 3–26 weeks. The animals were sacrificed after 1, 2, 3, 4, 6 and 24 weeks of administration of a 5% alcohol-containing liquid or a pair-fed control diet. The body weights of the control and alcohol rats increased in parallel, indicating the absence of any starvation or malnutrition in the control and alcohol-fed rats (Figure 1). The mean liquid diet ingestion was 79.8 ± 2.4 ml/day in the alcohol-fed rats for an ethanol intake of 12.94 g/kg/day. The incidences of ONFH in the control and the alcohol groups are shown in Table 1. No ONFH was observed in any rats fed with the control diet. In the control group, there was no change in the trabeculae or in the numbers of haematopoietic and fat cells. On the other hand, ONFH was observed in three of eight, four of eight and six of 12 rats, at 1, 2, 3 and 4 weeks respectively, after alcohol feeding. The incidence of ONFH in the 4-week alcohol rats was significantly higher than that in the 4-week control rats ($P = 0.0137$; Fisher's exact test). Figures 2 and 3 show the histopathological appearance of the femoral head after haematoxylin and eosin staining in typical experiments. Empty lacunae within the necrotic bone trabeculae, bone marrow cells including adipocytic necrosis and an accumulation of cell debris in the medullary space in most areas of the femoral head were observed at 1–3 weeks in the alcohol group. Feeding with the alcohol liquid diet for 4 weeks resulted in the formation of appositional bone around the necrotic bone trabeculae and, as part of the repair process, the deposition of fibrous and granulation tissue in the medullary space (Figures 2 and 3). Moreover, the repair process was more advanced in the alcohol group at 6 and 24 weeks, with the necrotic bone trabeculae observed to be surrounded by appositional bone. Additionally, partial appositional bone thickening of the bone trabeculae and normal haematopoietic and fat cells were observed in the alcohol group. These histopathological findings were observed in two of six and two of five rats in the alcohol group at 6 and 24 weeks respectively.

In the control rats, the liver had the expected regular chord-like architecture, whereas the liver in the alcohol-fed rats showed mild disorganization of the hepatic chord architecture and hepatocellular microsteatosis without necrosis, which progressed with time (Figure 4).

Figure 5 shows the blood concentrations of AST, ALT, TG, TC and HDL. All the parameters except TG were significantly higher in the alcohol group than in the control group from 1 week to 24 weeks. No significant changes were observed in blood IFNα levels at 1–6 weeks (Figure 5).

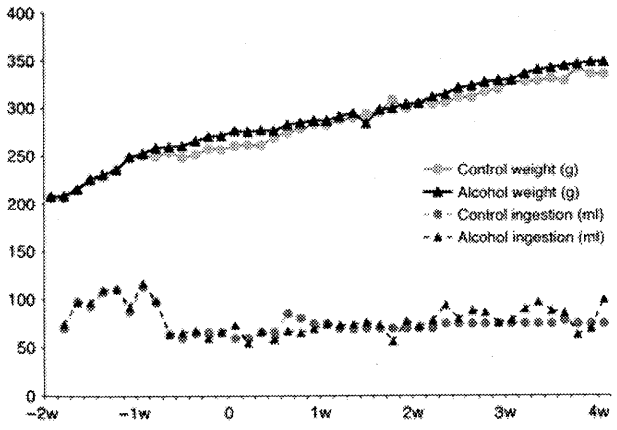

Figure 1 Changes in body weight and ingestion in the control and alcohol liquid diet–fed rats. The body weights of the control and alcohol rats increased in parallel.

Table 1 Incidence of osteonecrosis of the femoral head (ONFH) in the control and alcohol groups

	Feeding interval (week)				
Group	1	2	3	4	6
Control	0/8	0/8	0/8	0/12	0/6
Alcohol	3/8	3/8	4/8	6/12*	2/6

*$P = 0.0137$ *vs.* control by Fisher's exact test.

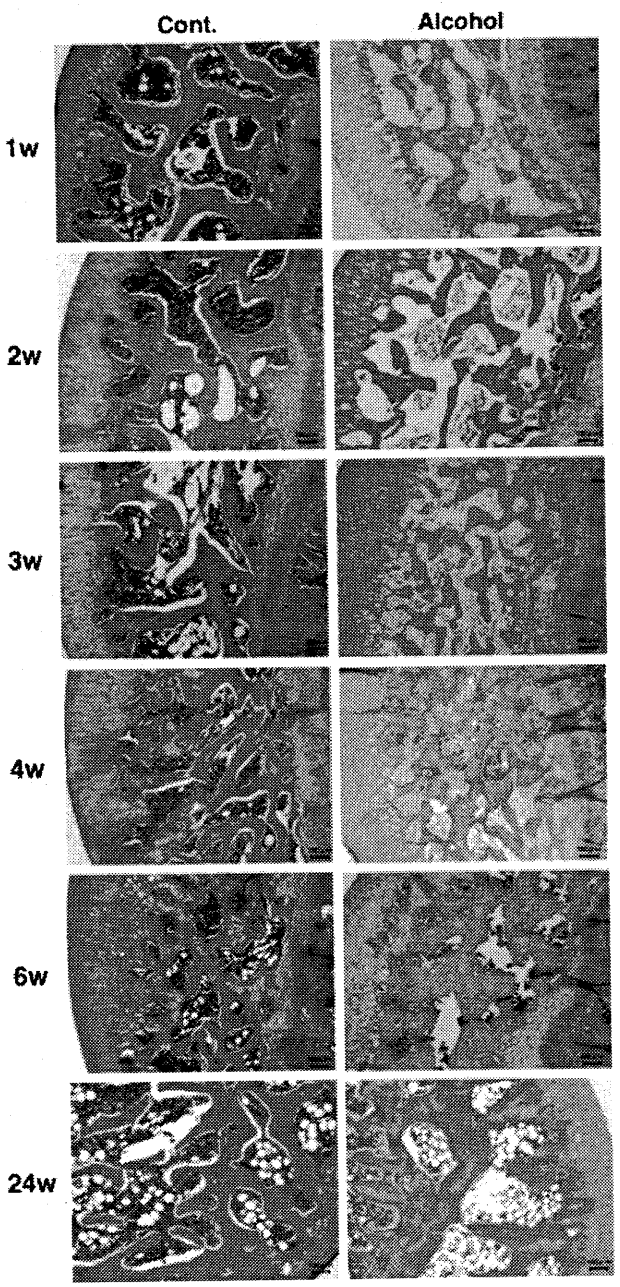

Figure 2 Histological appearance (low magnification) of the femoral head after haematoxylin and eosin staining in typical experiments. The alcohol group rats show the presence of diffuse empty lacunae in the bone trabeculae and bone marrow cell necrosis in most areas of the femoral head. The control group shows normal trabeculae and normal hematopoietic and fat cells over time. Scale bar represents 100 μm.

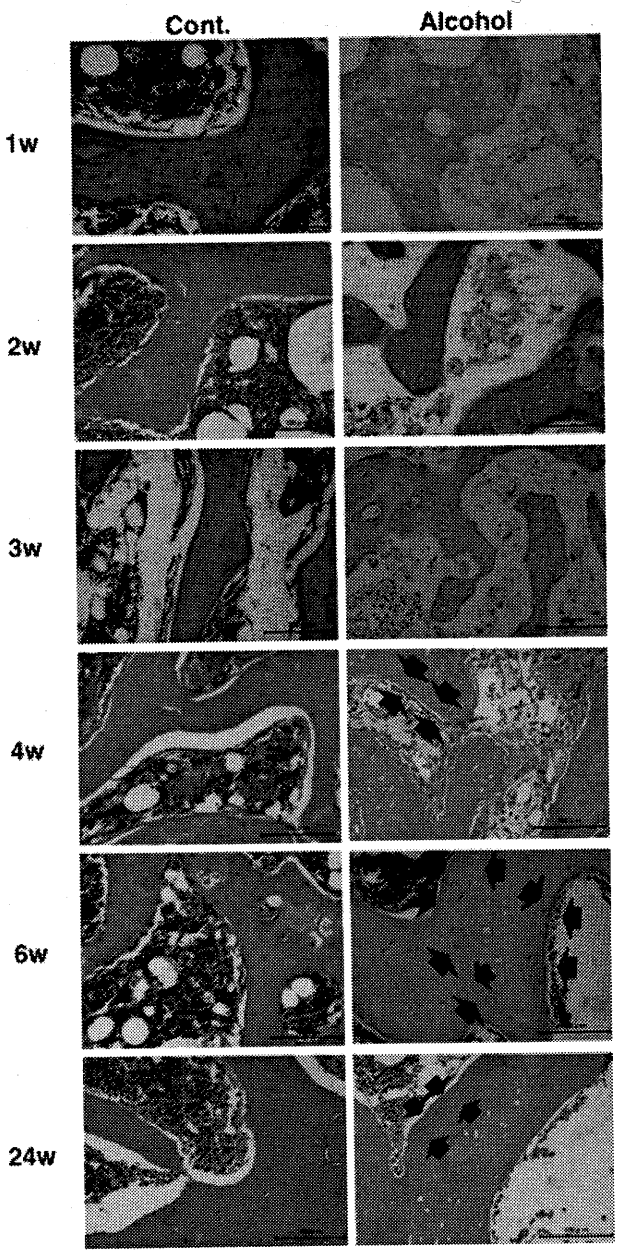

Figure 3 Histological appearance (high magnification) of the femoral head after haematoxylin and eosin staining. The alcohol group rats show the formation of appositional bone around necrotic bone trabeculae, which represents part of the repair process, at 4, 6 and 24 weeks (black arrow). Scale bar presents 100 μm.

Adiponectin was significantly lower at 1–4 weeks in the alcohol group than in the control group (Figure 5). On the other hand, no cytokines regulated by TLR signalling, such as IL-1α, IL-1β, IL-17 and IFNγ, were detected in either group (Data not shown). NF-κB activity did not significantly change at 1, 3 and 24 weeks, but was significantly decreased at 2 weeks in the alcohol group and significantly increased at 4 and 6 weeks in the alcohol group. On the other hand, the activity of IRF3 significantly changed only after 3 weeks of alcohol consumption. IRF7 activity also showed a significant change at 4 weeks in the alcohol-fed rats. Glutathione peroxidase activity in the liver was significantly increased at 2 and 4 weeks in the alcohol group, but was

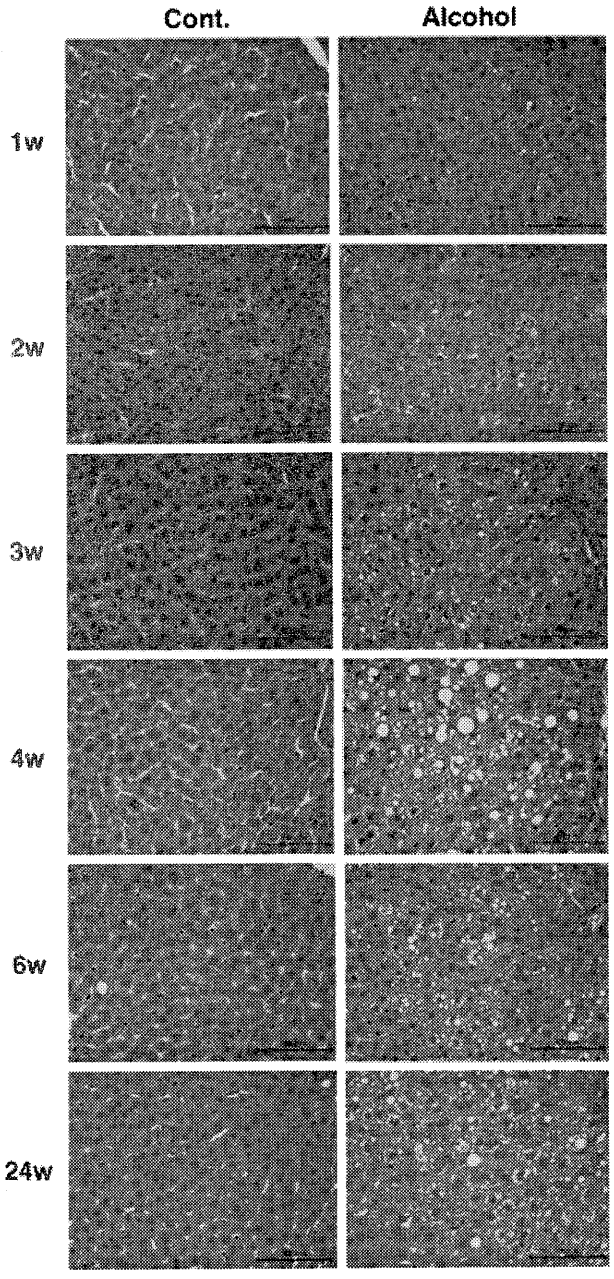

Figure 4 Histological appearance of the liver in the control and alcohol-fed rats. Control group rats show the expected regular chord-like architecture over time. The alcohol group rats show mild and moderate hepatocellular microsteatosis without necrosis. Scale bar represents 100 μm.

significantly decreased at 6 weeks in the alcohol group (Figure 6).

Discussion

In the present study, we found that feeding an alcohol liquid diet induced ONFH in rats. There have been a few reports on alcohol-induced ONFH in animal models; however, those models take 4–6 months to develop osteonecrosis through the administration of alcohol containing >45% ethanol intragastrically daily (Wang *et al.* 2003, 2008). In contrast, the present study showed that ONFH developed in rats fed with the 5% ethanol-containing liquid diet for 1 week, suggesting that ONFH can be initiated in a period as short as 7 days after feeding the animals with a 5% ethanol-containing liquid diet. Clinically, ONFH is observed in patients with a long-term history of drinking (Hirota *et al.* 1993). However, the precise time of onset of alcohol-induced ONFH in long-term drinkers remains unclear. The reasons for this include the fact that the collapse of the femoral head in humans may occur several months to years after the initial development of ONFH and may not show any symptoms until collapse (Mont *et al.* 2010).

The Lieber–DeCarli diet used in the present study is known to induce experimental alcoholic fatty liver disease (Lieber & DeCarli 1982; Lieber *et al.* 1989). The advantage of using this diet in animal experiments is that it allows the efficient consumption of ethanol (Lieber & DeCarli 1982; Lieber *et al.* 1989). In the present study, ONFH was observed within 7 days from the start of feeding with the 5% ethanol-containing liquid diet. This finding suggests that the alcohol-induced ONFH in humans may develop very early in drinkers with excessive alcohol consumption.

There have been some reports of changes in the histopathological findings of the femur induced by alcohol administration in animals. Solomon and Ikemura *et al.* reported that alcohol administration induced fatty bone marrow, but not osteonecrosis (Solomon 1985; Ikemura *et al.* 2011). Wang *et al.* reported that alcohol administration also induced fatty bone marrow and increased the percentage of empty lacunae as an index of osteonecrosis (Wang *et al.* 2008). However, we could not find any experimental reports on appositional bone formation as part of the repair process of bone necrosis after alcohol administration. Clinically, the detection of a band pattern on a magnetic resonance image is an important early finding for the diagnosis of non-traumatic ONFH and histopathologically corresponds to the repair tissue formed in cases of osteonecrosis (Bullough & DiCarlo 1990; Arlet *et al.* 1993; Sugano *et al.* 1999). The histopathological findings in the present study were very similar to those in patients with ONFH (Bullough & DiCarlo 1990; Arlet *et al.* 1993). We observed empty lacunae within the necrotic bone trabeculae and bone marrow cells including adipocytic necrosis in most areas of the femoral head in the alcohol group; results were similar to those observed in corticosteroid-induced ONFH model treated with corticosteroids after the administration of a TLR4 ligand, LPS (Okazaki *et al.* 2012). In particular, histological examination of the epiphysis showed osteocytic death and necrotic bone marrow with or without appositional bone. On the other hand, we did not observe any collapse of the femoral head in the rats fed an alcohol diet over 24 weeks. It was a difference between human and rat that the femoral head did not collapse. However, we reported that the initial

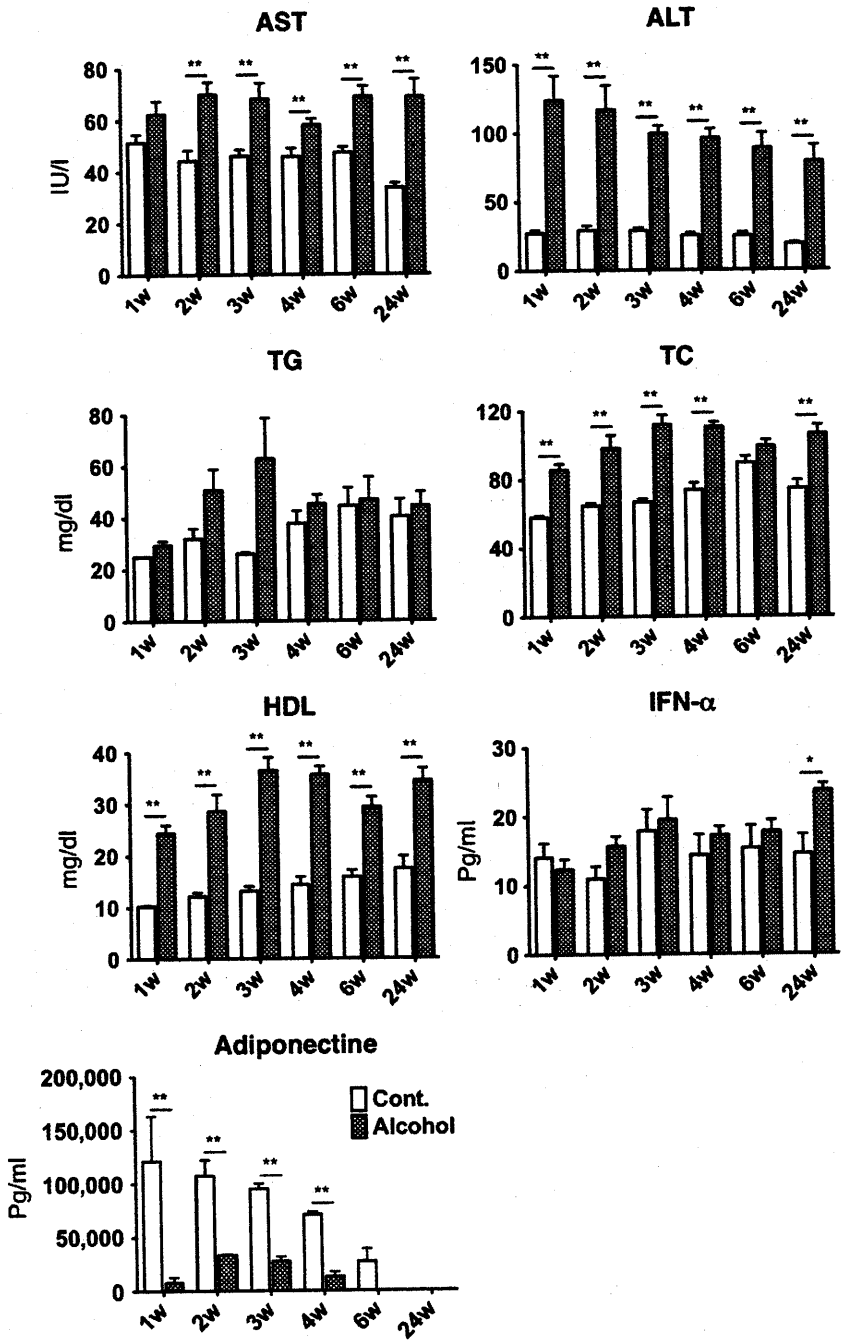

Figure 5 Increases in blood concentrations of AST, ALT, TG, TC and HDL and changes in blood IFNα and adiponectin levels in rats. AST, ALT, TC and HDL were significantly increased in the alcohol group over time. IFNα was not significantly changed in the alcohol group at 1–6 weeks, while the adiponectin level was significantly decreased in the alcohol group at 1–4 weeks. $*P < 0.05$ as control, $**P < 0.01$ as control.

development of ONFH and the collapse formation in the rat become independent and may not influence to elucidate the pathogenesis of ONFH (Okazaki *et al.* 2012). Therefore, our results suggest that this rat model could be used to unravel the underlying mechanisms of human ONFH. However, it should be noted that the structure of the femoral head differs between rats and humans. The epiphyseal line in the rat femur remains throughout adulthood (Okazaki *et al.* 2009). Focal ischaemia or thrombosis could not be observed in the proximal femur of the ONFH rats in the present study.

Enomoto *et al.* 1999 reported that chronic alcohol administration induces an increase in gut permeability resulting in elevated portal endotoxin levels. Endotoxin, a TLR4 ligand,

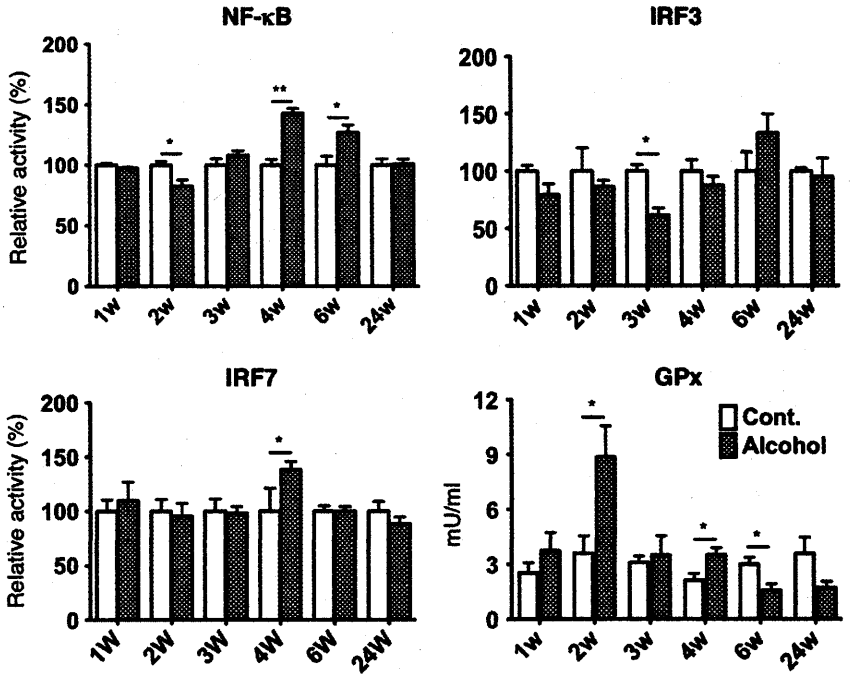

Figure 6 Activity of transcription factors NF-κB, IRF3 and IRF7, and GPx activity in the liver. NF-κB activity was significantly decreased at 2 weeks and was significantly increased at 4 and 6 weeks. IRF3 activity was significantly decreased at 3 weeks, and IRF7 activity was significantly increased at 4 weeks. GPx activity tended to be higher in the alcohol group than in the control group at 1–4 weeks. $*P < 0.05$ as control, $**P < 0.01$ as control.

induces a pro-inflammatory response via the TLR4 signalling pathway (Akira & Takeda 2004). We confirmed that NF-κB, IRF3 and IRF7, which are downstream transcriptional factors of the TLR4 signalling pathway, were activated in the liver during chronic alcohol consumption (Figure 6). However, we could not observe any activation of NF-κB, IRF3 or IRF7 in the liver at one week, i.e. the time at which the OFNH was first observed. And we could not observe any activation of pro-inflammatory cytokines regulated by TLR4 signalling. Therefore, whether the TLR4 signalling is associated with the initiation of alcohol-induced ONFH remains unclear. On the other hand, hypercholesterolaemia and hepatic steatosis were observed in the rats fed the alcohol liquid diet in the present study. We previously reported that hypercholesterolaemia and hepatic steatosis were also observed in corticosteroid-induced ONFH rat model after corticosteroid treatment (Okazaki *et al.* 2009). Further, previous clinical studies have reported an association between hyperlipidaemia and ONFH (Moskal *et al.* 1997; Kabata 2005). Therefore, hypercholesterolaemia may be related to the development of ONFH. Ichiseki *et al.* reported that administration of an oxidative stressor induced ONFH in rats and demonstrated that glutathione level acts as an index of oxidative stress-induced changes in the liver (Ichiseki *et al.* 2011). However, we could not observe any significant activation of GPx activity in the liver at 1 week, but we could observe any increase in transaminase levels in the fatty liver of rats fed the alcohol liquid diet. These findings suggest that any liver damage may contribute to the development of ONFH.

In the present study, adiponectin was significantly decreased in the alcohol group at 1, 2, 3 and 4 weeks, which is consistent with the findings of previous reports (You *et al.* 2005; Breitkopf *et al.* 2009). Hypoadiponectinaemia is associated with mortality following ischaemic stroke (Nishimura *et al.* 2007), and it has been suggested that it could be used as a biomarker for ischaemic stroke (Urbonaviciene *et al.* 2010). Therefore, the low adiponectin levels observed in the present study suggest the hypothesis that ONFH results from ischaemia of the femoral head.

In conclusion, we have developed a new rat model of alcohol-induced ONFH based on the feeding of an ethanol liquid diet, whereas it remains unclear whether the pro-inflammatory response via TLR4 signalling contributes to the development of alcohol-induced ONFH in rats fed with an ethanol liquid diet. This rat model will help us to unravel the underlying mechanisms of human ONFH.

Funding source

This work was supported in part by Grants-in-Aid for Young Scientists (B) (S.O., 22791390) and for Scientific Research (B) (H.M., 20390196) of the Japanese Society for the Promotion of Science.

Conflict of interest

The authors have no conflict of interests to declare.

References

Abeles M., Urman J.D., Rothfield N.F. (1978) Aseptic necrosis of bone in systemic lupus erythematosus. Relationship to corticosteroid therapy. *Arch. Intern. Med.* **138**, 750–754.

Akira S. & Takeda K. (2004) Toll-like receptor signalling. *Nat. Rev. Immunol.* **4**, 499–511.

Arlet J., Laroche M., Soler R., Thiechart M., Pieraggi M.T., Mazieres B. (1993) Histopathology of the vessels of the femoral heads in specimens of osteonecrosis, osteoarthritis and algodystrophy. *Clin. Rheumatol.* **12**, 162–165.

Breitkopf K., Nagy L.E., Beier J.I., Mueller S., Weng H., Dooley S. (2009) Current experimental perspectives on the clinical progression of alcoholic liver disease. *Alcohol. Clin. Exp. Res.* **33**, 1647–1655.

Bullough P.G. & DiCarlo E.F. (1990) Subchondral avascular necrosis: a common cause of arthritis. *Ann. Rheum. Dis.* **49**, 412–420.

Enomoto N., Yamashina S., Kono H. *et al.* (1999) Development of a new, simple rat model of early alcohol-induced liver injury based on sensitization of Kupffer cells. *Hepatology* **29**, 1680–1689.

Hirota Y., Hirohata T., Fukuda K. *et al.* (1993) Association of alcohol intake, cigarette smoking, and occupational status with the risk of idiopathic osteonecrosis of the femoral head. *Am. J. Epidemiol.* **137**, 530–538.

Hritz I., Mandrekar P., Velayudham A. *et al.* (2008) The critical role of toll-like receptor (TLR) 4 in alcoholic liver disease is independent of the common TLR adapter MyD88. *Hepatology* **48**, 1224–1231.

Ichiseki T. (2006) Oxidative stress by glutathione depletion induces osteonecrosis in rats. *Rheumatology* **45**, 287–290.

Ichiseki T., Kaneuji A., Ueda Y. *et al.* (2011) Osteonecrosis development in a novel rat model characterized by a single application of oxidative stress. *Arthritis Rheum.* **63**, 2138–2141.

Ikemura S., Yamamoto T., Motomura G. *et al.* (2011) Lipid metabolism abnormalities in alcohol-treated rabbits: a morphometric and haematologic study comparing high and low alcohol doses. *Int. J. Exp. Pathol.* **92**, 290–295.

Kabata T. (2005) Onset of steroid-induced osteonecrosis in rabbits and its relationship to hyperlipaemia and increased free fatty acids. *Rheumatology* **44**, 1233–1237.

Lieber C.S. & DeCarli L.M. (1982) The feeding of alcohol in liquid diets: two decades of applications and 1982 update. *Alcohol. Clin. Exp. Res.* **6**, 523–531.

Lieber C.S., DeCarli L.M., Sorrell M.F. (1989) Experimental methods of ethanol administration. *Hepatology* **10**, 501–510.

Lucey M.R., Mathurin P., Morgan T.R. (2009) Alcoholic hepatitis. *N. Engl. J. Med.* **360**, 2758–2769.

Matsumoto H., Sato Y., Azumi J., Kato J., Niitsu Y., Tamaki K. (2002) Role of endotoxin in NF-kappaB activation by ethanol in rat hepatocytes. *Alcohol. Clin. Exp. Res.* **26**, 6S–10S.

McClain C.J., Song Z., Barve S.S., Hill D.B., Deaciuc I. (2004) Recent advances in alcoholic liver disease. IV. Dysregulated cytokine metabolism in alcoholic liver disease. *Am. J. Physiol. Gastrointest. Liver Physiol.* **287**, G497–502.

Mont M.A., Jones L.C., Hungerford D.S. (2006) Nontraumatic osteonecrosis of the femoral head: ten years later. *J. Bone Joint Surg. Am.* **88**, 1117–1132.

Mont M.A., Zywiel M.G., Marker D.R., McGrath M.S., Delanois R.E. (2010) The natural history of untreated asymptomatic osteonecrosis of the femoral head: a systematic literature review. *J. Bone Joint Surg. Am.* **92**, 2165–2170.

Moskal J.T., Topping R.E., Franklin L.L. (1997) Hypercholesterolemia: an association with osteonecrosis of the femoral head. *Am. J. Orthop. (Belle Mead NJ)* **26**, 609–612.

Nishimura M., Izumiya Y., Higuchi A. *et al.* (2007) Adiponectin prevents cerebral ischemic injury through endothelial nitric oxide synthase-dependent mechanisms. *Circulation* **117**, 216–223.

Okazaki S., Nishitani Y., Nagoya S., Kaya M., Yamashita T., Matsumoto H. (2009) Femoral head osteonecrosis can be caused by disruption of the systemic immune response via the toll-like receptor 4 signalling pathway. *Rheumatology* **48**, 227–232.

Okazaki S., Nagoya S., Tateda K. *et al.* (2012) Weight bearing dose not contribute to the development of osteonecrosis of the femoral head. *Int. J. Exp. Pathol.* **93**, 458–462.

Okazaki S., Nagoya S., Yamamoto M. *et al.* (2013) High risk of osteonecrosis of the femoral head in autoimmune disease patients showing no immediate increase in hepatic enzyme under steroid therapy. *Rheumatol. Int.* **33**, 51–55.

Solomon L. (1985) Mechanisms of idiopathic osteonecrosis. *Orthop. Clin. North Am.* **16**, 655–667.

Sugano N., Kubo T., Takaoka K. *et al.* (1999) Diagnostic criteria for non-traumatic osteonecrosis of the femoral head. A multicentre study. *J. Bone Joint Surg. Br.* **81**, 590–595.

Tateda K., Okazaki S., Nagoya S. *et al.* (2012) The suppression of TRIM21 and the accumulation of IFN-alpha play crucial roles in the pathogenesis of osteonecrosis of the femoral head. *Lab. Invest.* **92**, 1318–1329.

Urbonaviciene G., Frystyk J., Flyvbjerg A., Henneberg E.W., Lindholt J.S. (2010) Association of serum adiponectin with risk for cardiovascular events in patients with peripheral arterial disease. *Atherosclerosis* **210**, 619–624.

Wang Y., Li Y., Mao K., Li J., Cui Q., Wang G.J. (2003) Alcohol-induced adipogenesis in bone and marrow: a possible mechanism for osteonecrosis. *Clin. Orthop. Relat. Res.* **410**, 213–224.

Wang Y., Yin L., Li Y., Liu P., Cui Q. (2008) Preventive effects of puerarin on alcohol-induced osteonecrosis. *Clin. Orthop. Relat. Res.* **466**, 1059–1067.

Yamamoto T., Irisa T., Sugioka Y., Sueishi K. (1997) Effects of pulse methylprednisolone on bone and marrow tissues: corticosteroid-induced osteonecrosis in rabbits. *Arthritis Rheum.* **40**, 2055–2064.

You M., Considine R.V., Leone T.C., Kelly D.P., Crabb D.W. (2005) Role of adiponectin in the protective action of dietary saturated fat against alcoholic fatty liver in mice. *Hepatology* **42**, 568–577.

Forensic Science International 231 (2013) 190–194

Contents lists available at SciVerse ScienceDirect

Forensic Science International

journal homepage: www.elsevier.com/locate/forsciint

Postmortem computed tomography lung findings in fatal of hypothermia

Hideki Hyodoh [a,*], Satoshi Watanabe [a], Ryuichi Katada [a], Kazusa Hyodoh [b], Hiroshi Matsumoto [a,c]

[a] Department of Legal Medicine, Sapporo Medical University, School of Medicine, S1 W17 Chuo-ku, Sapporo 060-8556, Japan
[b] Diagnostic Radiology, JR Sapporo Hospital, N3E1 Chuo-ku, Sapporo 060-0033, Japan
[c] Department of Legal Medicine, Osaka University Graduate School of Medicine, 2-2 Yamadaoka, Suita, Osaka 565-0871, Japan

ARTICLE INFO

Article history:
Received 11 June 2012
Received in revised form 10 May 2013
Accepted 13 May 2013
Available online 8 June 2013

Keywords:
Postmortem
Fatal hypothermia
CT
Lung

ABSTRACT

To identify lung findings specific to fatal hypothermia on postmortem computed tomography (CT) imaging.

Whole body CT scans were performed followed by full autopsy to investigate causes of death. There were 13 fatal hypothermia cases (group A) and 118 with other causes of death (group B). The chest cavity (CC), dead space including fluid/pneumothorax (DS), aerated lung volume (ALV), percentage aerated lung (%ALV), and tracheal aerated volume (ATV) were measured. Autopsy findings of groups A and B were compared. Receiver operating characteristics (ROC) curves were used to identify factors specific to fatal hypothermia.

There were no differences in age, sex, number with emphysema, or time from death to CT examination between the 2 groups. CC, DS, ALV, %ALV, and ATV were 2601.0 ± 247.4 (mL), 281.1 ± 136.5 (mL), 1564.5 ± 281.1 (mL), 62.1 ± 6.2 (%), and 21.8 ± 2.7 (mL) in group A and 2339.2 ± 67.7 (mL), 241.1 ± 38.0 (mL), 739.9 ± 67.0 (mL), 31.4 ± 2.3 (%), and 15.9 ± 0.8 (mL) in group B, respectively. There were statistically significant differences between groups A and B in ALV, %ALV and ATV. The multiple comparison procedure revealed that ALV and %ALV differed significantly between fatal hypothermia and other causes of death ($p < 0.05$). Using ROC evaluation, %ALV had the largest area under the curve (0.819).

This study demonstrates that the %ALV is greater in fatal hypothermia cases than in those with other causes of death on postmortem CT chest imaging. Based on CT, hypothermia is very likely to be the cause of death if the %ALV is >70%.

1. Introduction

As rates of conventional autopsy decline worldwide [1], postmortem computed tomography (CT) is increasingly performed to obtain supplementary or complementary information. Legally, postmortem CT imaging is useful as a non-destructive evaluation with and without traditional autopsy investigation. Thali et al. [2] conducted postmortem CT imaging with surface inspection, a technique reported as Virtopsy®. In emergency medicine, whole body scanning effects resuscitation aimed at survival, and whole body CT imaging is a routine process for evaluating trauma patients in emergency care settings [3]. CT imaging is usually performed to provide more detailed information than conventional X-rays and more objective information than other imaging techniques. CT has the added advantage that it can be scheduled with short notice. Because of these characteristics, postmortem CT imaging is applied to clarify cause of death in the emergency department and facilitate determining the need for autopsy, making it among the key imaging techniques described in a recent report [4].

This form of CT imaging allows us to assess postmortem changes including hypostasis in the heart [4], lungs [5], a hyperattenuated aortic wall [6], intra-vascular air [7,8], and dilatation of the right heart [7]. Additionally, postmortem findings show variable time-dependent changes [9,10], which can have special legal significance. However, these postmortem changes are not evident with all causes of death, and postmortem CT findings may not differ from those of pre-mortem CT imaging. We hypothesized that a lack of postmortem changes may reflect the effects of specific causes of death and that this phenomenon should be taken

* Corresponding author. Tel.: +81 11 611 2111x2759; fax: +81 11 611 3935.
E-mail addresses: hyodoh@sapmed.ac.jp (H. Hyodoh), satwat36@sapmed.ac.jp (S. Watanabe), r.katada@sapmed.ac.jp (R. Katada), khyodoh@sapmed.ac.jp (K. Hyodoh), hmatsumo@sapmed.ac.jp (H. Matsumoto).

0379-0738/$ – see front matter © 2013 Elsevier Ireland Ltd. All rights reserved.
http://dx.doi.org/10.1016/j.forsciint.2013.05.011

into consideration when interpreting postmortem CT imaging data.

In our institution, a CT imaging system was installed for legal purposes in 2010, and all autopsy cases are evaluated by postmortem CT imaging. Our institution is located at a latitude more than 40° N, and the average temperature is below freezing in the winter season. In many cases, the cause of death is fatal hypothermia. Our literature review yielded no reports on postmortem CT imaging in fatal hypothermia. We thus aimed to assess the features of fatal hypothermia on postmortem CT imaging.

2. Materials and methods

This study was approved by our institutional ethics committee. From July 2010 to November 2011, we examined 200 consecutive bodies. All deaths were reported to County Coroners. After the bodies had been found, the coroners refrigerated (cold storage) them at 4 °C if any delay in autopsy was anticipated.

2.1. Imaging protocol

The bodies were removed from the refrigerator and transferred to our institute prior to autopsy. All bodies were imaged in sealed body bags in the supine position, with arms adjacent to the body. All bodies were examined with a 64-slice multi-detector CT scanner (Aquilion CX, Toshiba, Japan) using the following protocol. First session: neck to head; 120 kV, 300 mA, 1.0 s/rotation, pitch factor 0.641, configuration 0.5 × 32, reconstruction 0.5 mm, MPR (multiplanar reformation) image reconstruction 5 mm in axial, sagittal, and coronal sections. Second session: neck to foot; 120 kV, 50–400 mA (variable mA), 0.5 s/rotation, pitch factor 0.828, configuration 0.5 × 32, reconstruction 0.5 mm, MPR image reconstruction 7 mm in axial plane, 5 mm in sagittal and coronal planes. After postmortem CT examinations, we conducted surface inspections, tracheal fiberscopy, blood tests, and urine tests within 30 min. After image interpretation, a full autopsy was promptly performed by a board-certified forensic pathologist. In this series, all 200 bodies underwent full autopsy. Exclusion criteria were lung putrefaction, chest trauma, being less than 20 years of age at the time of death, and imaging artifacts.

2.2. Imaging analysis

All datasets were stored in DICOM format. DICOM data were transferred to a personal computer MacBookPro (Macintosh OS X 10.6.8) with OSIRIX (App v.3.9.4). Using manual plotting and the semiautomatic region of interest (ROI) selection tool, we measured the following volumes: chest cavity (CC) without mediastinum (distinguish at the level of segmental bronchi) (Fig. 1a), aerated lung volume (ALV) (Fig. 1b), dead space (DS) volume (volume of chest fluid and pneumothorax), and tracheal aerated volume (ATV). OSIRIX software has a semiautomatic measurement tool, and we used the following thresholds: from −700 to −1000 Hounsfield Units (HU) for ALV and from −950 to −1100 HU for ATV measurement. Using the following formula, we calculated the percentage aerated lung volume (%ALV):

$$\text{percentage-ALV (\%ALV)} = \frac{\text{ALV}}{\text{CC} - \text{DS volume}}.$$

2.3. Statistical analysis

To evaluate the characteristics of fatal hypothermia, we divided the cadavers into two groups: fatal hypothermia (group A) and other causes of death (group B). Additionally, to compare the effects of each factor on lung aeration, we statistically analyzed each of 7 causes of death: hypothermia, drowning, suffocation, trauma, cardiac failure, poisoning, and intracranial bleeding. We used JMP (SAS Institute Inc., ver 10.0.2) software with the Mann–Whitney *U*-test for comparisons between fatal hypothermia and the other causes of death, and the Bonferroni method and multivariate logistic regression analysis (covariates; age, gender, imaged day, CC, ALV, %ALV, ATV) to compare effects between factors. We also used SPSS (SPSS Inc, 14.0.0, 2005) for receiver operating characteristics (ROC) to evaluate each factor's degree of discrimination. Differences at $p < 0.05$ were considered significant.

3. Results

3.1. Subject backgrounds

We excluded 69 cadavers due to putrefaction ($n = 29$), major trunk trauma ($n = 25$), age (less than 20 years, $n = 10$), and imaging artifacts ($n = 5$). We assessed 131 bodies (male 76, female 55). The causes of death were confirmed by full autopsy; hypothermia ($n = 13$), drowning ($n = 23$), suffocation ($n = 18$), trauma ($n = 17$), cardiac failure ($n = 8$), poisoning ($n = 7$), intracranial bleeding ($n = 6$), hanging ($n = 5$), carbon monoxide poisoning ($n = 4$), ileus ($n = 3$), pneumonitis ($n = 3$), brain damage ($n = 3$), inflammation ($n = 3$), multiple organ failure ($n = 2$), aortic rupture ($n = 2$), pulmonary embolization ($n = 2$), liver damage ($n = 2$), malnutrition ($n = 2$), air embolization ($n = 1$), intestinal perforation ($n = 1$), burn ($n = 1$), hyperthermia ($n = 1$), and unknown ($n = 4$). The respective gender ratios, ages, and times from death to CT imaging were male 9/female 4, 23–86 (mean, 61.4) years, and 1–60 (mean, 8.2) days in group A, and male 67/female 51, 21–89 (mean, 57.5) years, and 0–180 (mean, 5.1) days in group B. There were no background differences between the two groups (Table 1). One body in group A and 23 in group B showed emphysematous change.

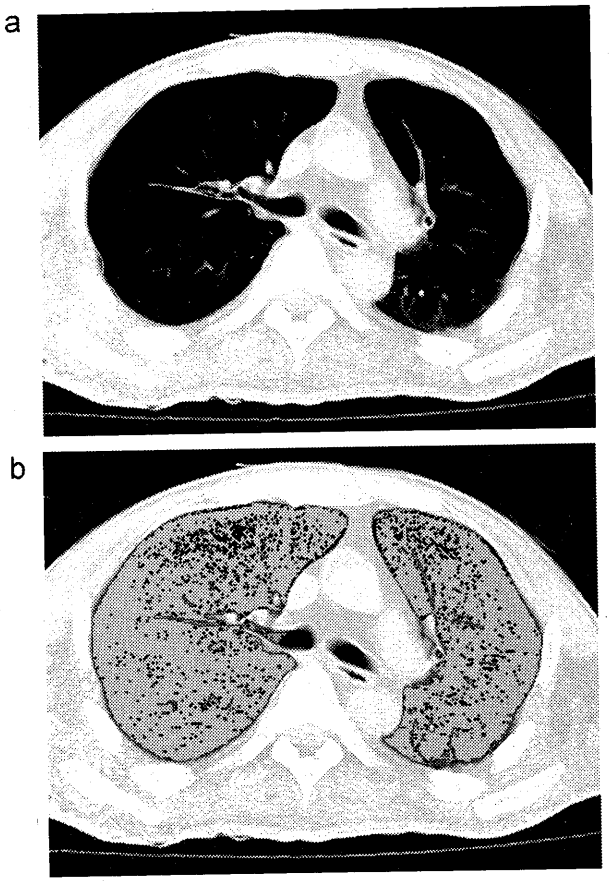

Fig. 1. (a) A 69-year-old man, cause of death: fatal hypothermia, 48 h after inquest. Using Osirix semi-automated program, CC (a) and ALV (b) were measured on postmortem CT. Then, %ALV was calculated employing the results obtained. (b) A 69-year-old man; cause of death, fatal hypothermia, 48 h after inquest Using Osirix semi-automated program, CC (a) and ALV (b) were measured on postmortem CT. Then, %ALV was calculated employing the results obtained. CC, 2183.8 mL; ALV, 1793.9 mL; %ALV, 82.1%; CC, chest cavity; ALV, aerated lung volume; %ALV, percent aerated lung volume.

Table 1
Background (Mann–Whitney *U*-test).

	Group A	Group B	*p*
Age (year)	23–86 (61.4)	21–89 (57.5)	0.4795
Sex (male:female)	9:4	67:51	0.3806*
Emphysema (yes:no)	1:12	23:105	0.3058
Time from death to CT (days)	8.2 ± 4.8	5.1 ± 1.6	0.0552

* χ^2 test.

Table 2
Statistical results (Mann–Whitney *U*-test).

	Group A	Group B	*p*
CC	2601.0 ± 247.4	2339.2 ± 67.7	0.2562
Dead space	281.1 ± 136.5	241.1 ± 38.0	0.6720
ALV	1564.5 ± 281.1	739.9 ± 67.0	0.0017
%ALV	62.1 ± 6.2	31.4 ± 2.3	0.0002
ATV	21.8 ± 2.7	15.9 ± 0.8	0.0439

CC, chest cavity (mL); ALV, aerated lung volume (mL); %ALV, percent aerated lung volume (%); ATV, aerated tracheal volume (mL).

3.2. Fatal hypothermia characteristics

CC, DS including fluid/pneumothorax, ALV, %ALV, and ATV were 2601.0 ± 247.4 (mL), 281.1 ± 136.5 (mL), 1564.5 ± 281.1 (mL), 62.1 ± 6.2 (%), and 21.8 ± 2.7 (mL), respectively, in group A and 2339.2 ± 67.7 (mL), 241.1 ± 38.0 (mL), 739.9 ± 67.0 (mL), 31.4 ± 2.3 (%), and 15.9 ± 0.8 (mL), respectively, in group B. There were statistically significant differences between groups A and B in ALV ($p = 0.0017$), %ALV ($p = 0.0002$), and ATV ($p = 0.0439$) (Table 2). As to postmortem imaging characteristics related to cause of death, fatal hypothermia cases had higher ALV and %ALV than those with other causes of death (Table 3, Fig. 2). The multivariate logistic regression analysis revealed %ALV to be the only statistically significant variable ($p = 0.014$, 95% confidence intervals 79–97%). The ROC evaluation revealed ALV and %ALV to be 0.766 and 0.815 for the area under the ROC curve with 95% confidence intervals from 0.653 to 0.879 and from 0.715 to 0.915, respectively (Fig. 3). Additionally, the 70% cut-off value for %ALV had a sensitivity of 0.462 and specificity of 0.907 (Table 4).

4. Discussion

Hypothermia is defined as a drop in core body temperature (under 35 °C). The body cannot generate enough heat to maintain a normal core body temperature, and organs malfunction [11]. Hypothermia has been recognized since the 19th century and is widely acknowledged to occur not only in individuals exposed to extreme environmental conditions, such as mountaineers, but even to those in temperate climates [12]. During the 1979–2002 period, a total of 16,555 death certificates in the United States had hypothermia-related diagnoses, and an average of 689 per year (range, 417–1021) were attributed to exposure to excessive natural cold [13].

Pulmonary hypostasis develops during the first few postmortem hours [14]. The pressure gradient between the pulmonary vasculature and the alveolar space [15,16], and altered capillary permeability are responsible for hypostasis in the postmortem period. Dependent density in the lungs has been shown to be a nonspecific postmortem CT finding, and hypostasis would be more severe in the dependent position [5]. This density increases with the passage of time [17] on postmortem CT imaging. We found lung and tracheal aeration to be preserved on postmortem CT imaging in fatal hypothermia cases. Our study showed that when hypothermia is the cause of death, pulmonary hypostasis does not develop (or is less severe than that with other causes of death), and that pulmonary aeration is preserved as compared with other causes of death. To the best of our knowledge, this is the first report documenting this novel finding.

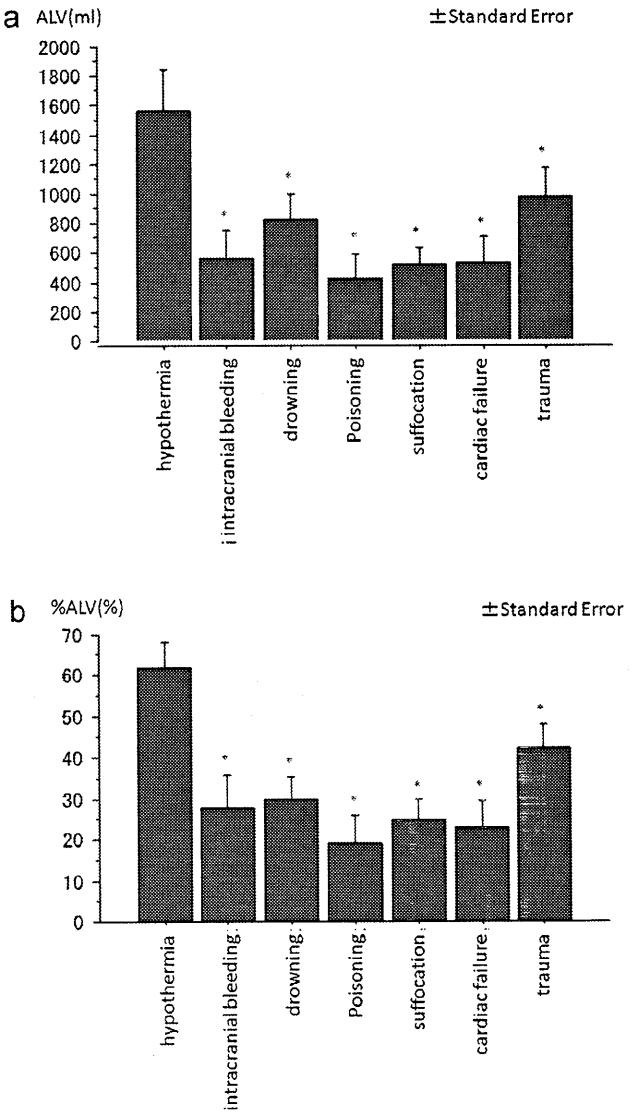

Fig. 2. (a) Characteristics of causes of death; ALV Fatal hypothermia was associated with significantly higher ALV (a) and %ALV (b) than the six other causes of death examined (*$p < 0.05$). (b) Characteristics of causes of death; %ALV fatal hypothermia was associated with significantly higher ALV (a) and %ALV (b) than the six other causes of death examined (*$p < 0.05$). ALV, aerated lung volume; %ALV, percent aerated lung volume.

Table 3
Comparison of other causes of death with fatal hypothermia (Bonferroni/Dunn's procedure).

	Drowning	Suffocation	Trauma	Cardiac failure	Poisoning	Intracranial bleeding
n	23	18	17	8	7	6
CC	0.5787	0.0049	0.6168	0.2968	0.1652	0.2090
Dead space	0.6851	0.1358	0.0014	0.8725	0.1684	0.6491
ALV	0.0058	0.0002	0.0379	0.0029	0.0017	0.0080
%ALV	0.0002	<0.0001	0.0300	0.0006	0.0003	0.0050
ATV	0.0046	0.0133	0.3880	0.1541	0.3552	0.0354

Control: fatal hypothermia ($n = 13$).
CC, chest cavity; ALV, aerated lung volume; %ALV, percent aerated lung volume; ATV, aerated tracheal volume.

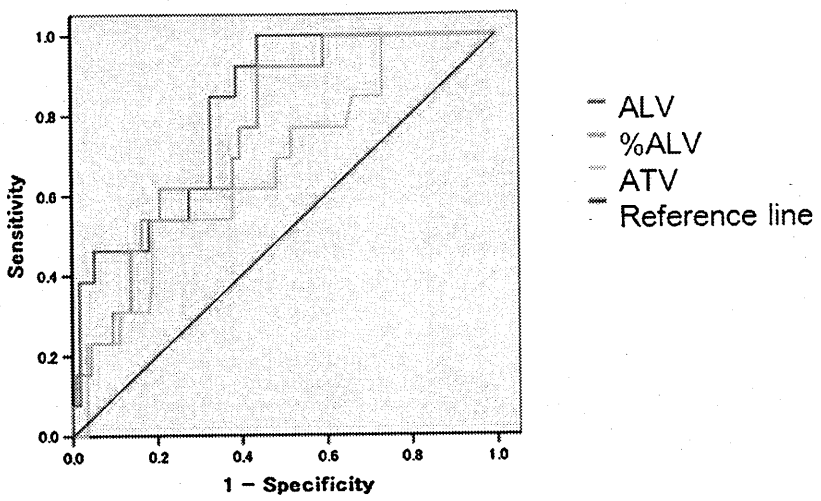

Test Result Variable(s)	Area	Std.Error	Asymptotic Sig.	Asymptotic 95% Confidence Interval	
				Lower Bound	Upper Bound
ALV	.766	.058	.002	.653	.879
%ALV	.816	.051	.000	.717	.916
ATV	.671	.076	.044	.521	.820

Fig. 3. Receiver operating characteristics (ROC) curve. Based on ROC evaluation, ALV and %ALV had areas under the curve of 0.766 and 0.815 with 95% confidence intervals from 0.653 to 0.879 and from 0.715 to 0.915, respectively. ALV, aerated lung volume; %ALV, percent aerated lung volume; ATV, aerated tracheal volume.

Fatal hypothermia can be assessed employing characteristic autopsy findings, such as low rectal temperature, the cherry sign, right/left cardiac blood color difference, blood coagulability [18], Wischnevsky's gastric ulcer [18], increased urinary bladder volume [18], and iliopsoas intramuscular bleeding [19,20], without other evidence of causes of death. In our study, ALV, %ALV, and ATV differed significantly between hypothermia and other causes of death while other factors did not. According to our ROC evaluation, the %ALV differed most markedly in this series. Therefore, high %ALV might be a finding specific to fatal hypothermia on postmortem CT imaging.

Henzler et al. reported that normal aerated lung CT values ranged from −700 to −900 HU [21]. Our estimated aerated lung CT values were from −700 to −1000 HU. If we apply a wider measurement range, ALV may increase but this might include areas of poorly aerated lung. The assignment of different density ranges to ALV could thus alter results [21]. For ATV measurement, we use −950 HU as the minimum HU value because of the 5% error in air density.

Shiotani et al. reported that delayed postmortem CT showed time-dependent opacity and the appearance of consolidation, corresponding to congestive pulmonary edema [9]. They did not, however, maintain the corpses they studied in cold storage, and this may have increased lung-dependent opacity and consolidation. In the present series, as imaging time increased after inspection, %ALV remained high when hypothermia was the cause of death but not when other causes were documented. We found lung edematous change/hypostasis to be less frequent under hypothermic conditions. We speculate that pulmonary congestion/edema is less common in fatal hypothermia than with other causes of death and that lung aeration is maintained by the hypothermic condition. We also hypothesized that when life ceases due to fatal hypothermia, if the body is stored at a warm temperature, lung edema/hypostasis increases with the passage of time. As more time passes, putrefaction may affect the corpse.

In the postmortem period, the lung usually develops edema/hypostasis which increases the CT value, while fatal hypothermia is associated with marked maintenance of lung aeration and low attenuation on CT images. Herein, we showed %ALV to be much greater in fatal hypothermia than with other causes of death on postmortem CT imaging. This high %ALV was a good indicator of fatal hypothermia. As this is a newly recognized postmortem CT imaging finding of fatal hypothermia, it may serve as an index allowing fatal hypothermia to be distinguished from other causes of death. Further prospective studies are needed to verify this novel finding.

Prior to postmortem CT imaging, lung pathological conditions may affect postmortem changes. Thus, it is important to consider basal disease effects on postmortem imaging. In our series, if emphysematous change was present, lung attenuation was often decreased, and %ALV would thus tend to be increased. There were no statistically significant differences in background factors between fatal hypothermia and other causes of death, but special consideration is needed in the interpretation of individual postmortem imaging findings. On the other hand, if pneumonia

Table 4
%ALV cut-off value and sensitivity/specificity for diagnosis of the fatal hypothermia.

%ALV cut-off value (%)	Sensitivity	Specificity
40	0.846	0.644
50	0.538	0.746
60	0.462	0.856
70	0.462	0.907
80	0.385	0.975

%ALV, percent aerated lung volume.

was a basal condition, lung aeration and the infectious pulmonary lesions were preserved as in the pre-mortem state, such that %ALV was decreased. Therefore, when applying the %ALV determined from postmortem CT imaging, we must consider basal conditions which can increase or decrease ALV. In other words, if the basal condition affects lung aeration, this may reduce the value of %ALV for determining whether or not hypothermia is the main cause of death.

The first limitation of our study is that causes of death have complex effects. We could not adequately evaluate the combination of drug poisoning and low temperature. We suspect that ALV might decrease with drug poisoning, but if the body is exposed to a low temperature before death there would be no evident effect on postmortem CT imaging. Second, the fatal hypothermia group consisted of only 13 cases (9.8%), and the other group was limited in variety. We need to collect data on other causes of death, especially malnutrition. This is because malnutrition might decrease caloric reserves, and would thus tend to present a condition similar to that of fatal hypothermia, also possibly decreasing the amount of bodily fluid, thereby reducing edematous lung change. Third, we evaluated only 7 causes of death (hypothermia, intracranial bleeding, drowning, poisoning, suffocation, cardiac failure, and trauma). The variety of subgroups was limited, and other factors might be associated with characteristic CT findings. Fourth, we excluded cases less than 20 years of age, such that our findings are not applicable to the pediatric population. We cannot expect the same results in children without further examination.

In conclusion, we retrospectively evaluated the postmortem CT imaging findings of autopsied cases and showed %ALV to be increased in those with fatal hypothermia. This is the first report on postmortem CT findings in fatal hypothermia. The %ALV index might aid in the investigation of cause of death for legal purposes.

References

[1] L. Patriquin, A. Kassarjian, M. Barish, L. Casserley, M. O'Brien, C. Andry, et al., Postmortem whole-body magnetic resonance imaging as an adjunct to autopsy: preliminary clinical experience, J. Magn. Reson. Imaging 13 (2001) 277–287.
[2] M.J. Thali, K. Yen, W. Schweitzer, P. Vock, C. Boesch, C. Ozdoba, et al., Virtopsy, a new imaging horizon in forensic pathology: virtual autopsy by postmortem multislice computed tomography (MSCT) and magnetic resonance imaging (MRI) – a feasibility study, J. Forensic Sci. 48 (2003) 386–403.
[3] S. Huber-Wagner, R. Lefering, L.M. Qvick, M. Korner, M.V. Kay, K.J. Pfeifer, et al., Effect of whole-body CT during trauma resuscitation on survival: a retrospective, multicentre study, Lancet 373 (2009) 1455–1461.
[4] S. Shiotani, M. Kohno, N. Ohashi, K. Yamazaki, Y. Itai, Postmortem intravascular high-density fluid level (hypostasis): CT findings, J. Comput. Assist. Tomogr. 26 (2002) 892–893.
[5] S. Shiotani, M. Kohno, N. Ohashi, K. Yamazaki, H. Nakayama, K. Watanabe, et al., Non-traumatic postmortem computed tomographic (PMCT) findings of the lung, Forensic Sci. Int. 139 (2004) 39–48.
[6] S. Shiotani, M. Kohno, N. Ohashi, K. Yamazaki, H. Nakayama, Y. Ito, et al., Hyperattenuating aortic wall on postmortem computed tomography (PMCT), Radiat. Med. 20 (2002) 201–206.
[7] S. Shiotani, M. Kohno, N. Ohashi, K. Yamazaki, H. Nakayama, K. Watanabe, et al., Dilatation of the heart on postmortem computed tomography (PMCT): comparison with live CT, Radiat. Med. 21 (2003) 29–35.
[8] N. Takahashi, T. Higuchi, M. Shiotani, H. Maeda, Y. Hirose, Intrahepatic gas at postmortem multislice computed tomography in cases of nontraumatic death, Jpn. J. Radiol. 27 (2009) 264–268.
[9] S. Shiotani, T. Kobayashi, H. Hayakawa, K. Kikuchi, M. Kohno, Postmortem pulmonary edema: a comparison between immediate and delayed postmortem computed tomography, Leg. Med. 13 (2011) 151–155.
[10] F. Fischer, J. Grimm, C. Kirchhoff, M.F. Reiser, M. Graw, S. Kirchhoff, Postmortem 24-h interval computed tomography findings on intrahepatic gas development and changes of liver parenchyma radiopacity, Forensic Sci. Int. 214 (2012) 118–123.
[11] Centers for Disease Control and Prevention (CDC), Hypothermia-related deaths – United States, 1999–2002 and 2005, Morb. Mortal. Wkly. Rep. 55 (2006) 282–284.
[12] E.E. Turk, Hypothermia, Forensic Sci. Med. Pathol. 6 (2010) 106–115.
[13] Centers for Disease Control and Prevention (CDC), Hypothermia-related deaths – United States, 2003–2004, Morb. Mortal. Wkly. Rep. 54 (2005) 173–175.
[14] S. Shiotani, K. Watanabe, M. Kohno, N. Ohashi, K. Yamazaki, H. Nakayama, Postmortem computed tomographic (PMCT) findings of pericardial effusion due to acute aortic dissection, Radiat. Med. 22 (2004) 405–407.
[15] L.W. Hedlund, P. Vock, E.L. Effmann, M.M. Lischko, C.E. Putman, Hydrostatic pulmonary edema. An analysis of lung density changes by computed tomography, Invest. Radiol. 19 (1984) 254–262.
[16] P. Scillia, M. Delcroix, P. Lejeune, C. Melot, J. Struyven, R. Naeije, et al., Hydrostatic pulmonary edema: evaluation with thin-section CT in dogs, Radiology 211 (1999) 161–168.
[17] F.S. Chew, A. Relyea-Chew, E.R. Ochoa Jr., Postmortem computed tomography of cadavers embalmed for use in teaching gross anatomy, J. Comput. Assist. Tomogr. 30 (2006) 949–954.
[18] M.L. Mallet, Pathophysiology of accidental hypothermia, QJM 95 (2002) 775–785.
[19] M. Ogata, K. Ago, M. Ago, T. Kondo, K. Kasai, T. Ishikawa, et al., A fatal case of hypothermia associated with hemorrhages of the pectoralis minor, intercostal, and iliopsoas muscles, Am. J. Forensic Med. Pathol. 28 (2007) 348–352.
[20] E. Aghayev, M.J. Thali, C. Jackowski, M. Sonnenschein, R. Dirnhofer, K. Yen, MRI detects hemorrhages in the muscles of the back in hypothermia, Forensic Sci. Int. 176 (2008) 183–186.
[21] D. Henzler, A.H. Mahnken, J.E. Wildberger, R. Rossaint, R.W. Gunther, R. Kuhlen, Multislice spiral computed tomography to determine the effects of a recruitment maneuver in experimental lung injury, Eur. Radiol. 16 (2006) 1351–1359.

厚生労働科学研究費補助金（循環器疾患・糖尿病等生活習慣病対策総合研究事業）
WHO 世界戦略を踏まえたアルコールの有害使用対策に関する総合的研究
（研究代表者　樋口　進）

平成 25 年度分担研究報告書
コンピューターを用いた簡易介入ツールの開発と有効性検証

研究分担者　杠　岳文　独立行政法人国立病院機構肥前精神医療センター　院長

研究要旨
簡易介入は、飲酒量低減指導の技法としてその有効性がすでに確立されている。現在、スマートフォンやタブレット端末をはじめ、コンピューターは我々の日常生活に深く浸透している。コンピューターには利用に関して時間や場所の制約がなく、プライバシーも保たれやすい。また、通常の簡易介入と異なり対面式ではなく、マンパワーも要しない。このようなコンピューターのメリットを活かし、コンピューター上で出来る飲酒量低減指導プログラムを開発、保健指導の場面などで活用し、その有効性を検証することを目的とする。

研究協力者
角南隆史：肥前精神医療センター精神科医師

A．研究目的

コンピューターを用いて、簡易介入の重要な構成要素とされる個人の飲酒習慣の評価及び飲酒に関する教育、そして飲酒量低減に向けた目標の設定、飲酒量の記録などを多量飲酒者自身が一人でできるプログラムを開発し、有効性の検証を行うものである。

海外では「check your drinking」、「down your drink」などで、コンピューター上で AUDIT を用いた個人の飲酒習慣の評価や教育、飲酒量の記録などを行うツールが開発されている。しかし日本では、アサヒビール(株)が「お酒 diary」としてコンピューター上で自らの飲酒量を記録しフィードバックされるツールが作成されているのみで、個人の飲酒習慣の評価や教育そしてそれに見合った目標設定を行うツールは作成されていない。われわれは、簡易介入のなかで行動変容に有効な構成要素を組み入れたプログラムを開発し、実際に保健指導などの場面で活用しながら、その有効性を検証する。

B．研究方法

①初年度：作成

スクリーニングテストを実施し、その評価を個別にフィードバックし、さらには多量飲酒による心身の健康障害に関する基礎知識を自己学習できるコンピュータープログラムを作成する。

②次年度：有効性の検証

上記プログラムを用いて職域や地域、医療機関において健診や健康フェスタなどの場面で使用し、参加者の反応を見ながらプログラムの改良を行い、有効性の検証を行う。さらには、飲酒日記を応用しコンピューター上でセルフモニタリングとそのフィードバックを行えるプログラムを作成する。

③最終年度：普及

プログラムの有効性の検証を行うとともに、作成した簡易介入の補助ツールの普及を簡易介入の研修の中で行う。そして上記プログラムをウェブ上にアップする。またウェブ上の自助グループについても検討する。その際には、とくにその適正な運用のための規程やマニュアルを作成する。

（倫理面への配慮）

介入のためのコンピュータープログラム

の開発であり、入力される情報も年代と性別であるため個人情報も保護されるものと考える。

C．研究結果

現在は初年度であり、B研究方法の①に記載したプログラムを現在作成中である。

D．考察

不適切な飲酒者と多量飲酒者に対する節酒指導はアルコール健康障害対策基本法の中でも重要な施策として掲げられている。簡易介入は、飲酒量低減指導の技法としてその有効性が主に医療現場においてすでに確立されている。一方、わが国においては、未だ介入カウンセラーの人材育成も進んでおらず、この介入技法の普及に至っていない。一方、コンピューターの普及は急速に進み、だれでも、どこでも利用できる状況になりつつある。また、コンピューターには利用に関して時間や場所の制約がなく、プライバシーも保たれやすい。さらに、簡易介入と異なり対面式ではなく、マンパワーも要しない。このようなコンピューターのメリットを活かし、コンピューター上で出来る飲酒量低減指導プログラムの開発に取り組んでいる。

厚生労働科学研究費補助金（循環器疾患・糖尿病等生活習慣病対策総合研究事業）
（分担）研究総合報告書

アルコール性肝障害の実態調査

分担研究者　堀江　義則　国際医療福祉大学臨床医学研究センター

研究要旨【背景】近年、アルコールの総消費量は若干の減少傾向を示しているが、女性飲酒者数は増加傾向にあり、問題飲酒者と判定される症例数も依然として300万人超と推計され、このような問題飲酒者の中から肝障害患者が高頻度に発症している。こうした本邦の現状を受け、平成25年12月にアルコール健康障害対策基本法が公布された。その第24条には、「国及び地方公共団体は、アルコール健康障害の発生、進行(中略)に関する実態調査その他の調査研究を推進するために必要な施策を講ずるものとする。」とあり、これに沿って肝硬変発症における飲酒の影響についての変遷を検討した。【方法】全国の日本消化器病学会認定、関連施設1390施設に対して平成24年度（平成24年4月～平成25年3月）に入院した肝硬変患者の成因についてのアンケートを実施し、平成10年ならびに19～20年度の全国調査のデータと比較した。【成績】9326例（男：5768、女：3558）の肝硬変患者についての回答があり、アルコール単独によるものは2293例, 24.6％（男：1979例, 34.3%、女：314例, 8.8%）で、肝炎ウイルスマーカー陽性例、自己免疫性例をあわせると2857例, 30.6％（男：2446例, 42.4%、女：411例, 11.6%）であった。【考察】平成10年度の調査では、全肝硬変患者のうちアルコール単独によるものは12%、平成19～20年度の調査では14%であるのに対し、今回の調査では24.6%と急速にその割合が上昇していた。特に男性でその傾向が顕著であった。肝炎ウイルスの関与については、平成19～20年度の調査ですでにウイルス性合併アルコール性肝硬変症例は平成10年度の15%から6%と激減していたが、今回の検討でも6%で、近年はアルコール性肝硬変への進展に肝炎ウイルスの影響は少ないと考えられた。全肝硬変患者のうちアルコール単独によるアルコール性肝硬変の割合が著明に増加しており、今後は基本法に基づいて国が策定する基本計画に沿って、問題飲酒者数そのものの低減を目指す必要がある。

A、緒言

戦後、わが国におけるアルコールの総消費量は著明な増加を示し、飲酒者数の増加のみならず、成人一人当たりのアルコール消費量も増加してきた。平成11年度をピークに総消費量は若干の減少傾向を示しているが、依然としてアルコール消費量は高い水準にあり、現代生活では飲酒は日常的行為で、個人の生活習慣を形成している重要な因子のひとつである。このようにアルコール性肝障害は、現代日本の飲酒状況を見ると生活習慣病と呼ぶにふさわしく、その中の重要な位置を占めていると考えられる。

わが国におけるアルコール性肝障害の全国調査の結果と国税庁酒税課による調査をもとに、肝疾患におけるアルコール性肝障害の比率と成人一人あたりのアルコール消費量の相関をみると、最近は成人一人あたりの飲酒量の増加は上げ止まったもの、年々肝疾患におけるアルコール性肝障害の比率は増加しており、2002年度には20%を超えて22.8%に達した。

また、近年女性飲酒者数は増加傾向にあり、問題飲酒者と判定される症例数も依然として300万人超と推計され、このような問題飲酒者の中から肝障害患者が高頻度に発症している。こうした本邦の現状を受け、平成25年12月にアルコール健康障害対策基本法が公布された。その第24条には、「国及び地方公共団体は、アルコール健康障害の発生、進行(中略)に関する実態調査その他の調査研究を推進するために必要な施策を講ずるものとする。」とあり、これに沿って肝硬変発症における飲酒の影響についての変遷を検討した。

B、方法

全国の日本消化器病学会認定、関連施設 1389 施設に対して平成 24 年度（平成 24 年 4 月～平成 25 年 3 月）に入院した肝硬変患者の成因についてのアンケートを行った。

C、結果

郵送対象施設数 1390 施設に対して、有効な回答のあった施設は 95 施設で、回答率は 6.8%であった。9326 例（男：5768、女：3558）の肝硬変患者についての回答があり、アルコール単独によるものは 2293 例, 24.6％（男：1979 例, 34.3%、女：314 例, 8.8%）で、肝炎ウイルスマーカー陽性例、自己免疫性例をあわせると 2857 例, 30.6 %（男：2446 例, 42.4%、女：411 例, 11.6%）であった（表、図）。

D、考察

アルコール性肝障害における肝炎ウイルスの関与については、平成 10 年度の全国 45 施設の調査によると、全肝硬変患者のうちアルコール単独によるものは 12.1%であるが、アルコール＋ウイルスによるものも含めると、アルコール多飲が関与する肝硬変は、27.1%に達した。平成 19-20 年度の結果ではアルコール単独のものは 14.0%と平成 10 年の 12.1%より微増しているのに対し、ウイルス性合併例は 15.0%から 6.3%と激減していた。医師会をはじめとする各種団体による市民公開講座やマスコミなどを通じた啓発活動により、肝炎ウイルス感染者の飲酒率、少なくとも日本酒換算で 3 合以上の常習飲酒者の割合が低下した可能性も示唆された。

しかし、今回の調査では純粋なアルコール性肝硬変患者の割合は、平成 19-20 年度の 13.7%から 24.6%、アルコール＋ウイルス性肝硬変を加えた肝硬変患者は 20.3%から 30.6%と著明に増加していた。（表、図）。

成人一人あたりの飲酒量の増加は上げ止まっているのに対し、以前の全国統計よりも肝硬変患者のうちアルコール性肝硬変患者の比率が増加した理由として、近年の人口の高齢化が関与している可能性もある。高齢化により常習飲酒期間が長期化し積算飲酒量が増加することが、肝硬変まで進展させ入院加療を必要とさせる可能性もある。また、平均的な飲酒者が減少し、機会飲酒者と大量飲酒者のように飲酒量の二極化が起こっている可能性もある。今後は基本法に基づいて国が策定する基本計画に沿って、問題飲酒者数そのものの低減を目指す必要がある。

E、結論

平成 10 年度の調査では、全肝硬変患者のうちアルコール単独によるものは 12%、平成 19～20 年度の調査では 14%であるのに対し、今回の調査では 24.6%と急速にその割合が上昇していた。特に男性でその傾向が顕著であった。肝炎ウイルスの関与については、平成 19～20 年度の調査ですでにウイルス性合併アルコール性肝硬変症例は平成 10 年度の 15%から 6%と激減していたが、今回の検討でも 6%で、近年はアルコール性肝硬変への進展に肝炎ウイルスの影響は少ないと考えられた。全肝硬変患者のうちアルコール単独によるアルコール性肝硬変の割合が著明に増加しており、今後は基本法に基づいて国が策定する基本計画に沿って、問題飲酒者数そのものの低減を目指す必要がある。

F、謝辞

今回のアンケート調査にご協力いただいた、下記の医療機関に対して、心より謝意を表します。

相澤病院　消化器科、赤磐医師会病院　内科、上尾中央総合病院　消化器内科、朝倉医師会病院　消化器内科、今村病院　肝臓内科、岩国医療センター　肝臓内科、磐田市立総合病院　消化器内科、岩手医科大学　消化器肝臓内科、永寿総合病院　消化器内科、小郡第一総合病院　内科、大阪医療センター　消化器内科、岡山済生会総合病院　肝臓病センター、香川大学　消化器・神経内科、化研病院　消化器内科、鹿児島市医師会病院　消化器内科、金沢医科大学　肝胆膵内科、川崎医科大

学　肝胆膵内科学、関西医科大学附属香里病院　内科、関西医科大学附属滝井病院　消化器肝臓内科、関西医科大学牧方病院、関東労災病院　消化器内科、菊川市立総合病院　内科、北里大学東病院　消化器内科、岐阜大学　第一内科、京都府立医科大学　消化器内科、京都府立医科大学北部医療センター　消化器内科、串間市民病院　内科、くまもと森都総合病院　肝臓・消化器内科、倉敷平成病院　消化器科、久留米大学　消化器内科、群馬大学附属病院　病態制御内科、慶應義塾大学病院　消化器内科、けいゆう病院　内科、県立広島病院　消化器内科、甲府共立病院　内科、済生会川口総合病院　消化器内科、済生会二日市病院　内科、埼玉医科大学　消化器内科・肝臓内科、埼玉協同病院　消化器内科、さいたま市民医療センター　消化器内科、佐賀大学　肝臓・糖尿病・内分泌内科、相模原病院　消化器内科、札幌道都病院　内科、産業医科大学若松病院　消化器内科、JA愛知厚生連海南病院　消化器内科、滋賀医科大学附属病院　消化器内科、昭和大学病院　消化器内科、市立長浜病院　消化器内科、信州上田医療センター、信州大学　消化器内科、鈴鹿回生病院　消化器内科、聖マリアンナ医科大学　消化器肝臓内科、総合大雄会病院　消化器内科、高崎総合医療センター　消化器内科、多根総合病院　消化器内科、千曲中央病院　内科、千葉西総合病院　消化器内科、中電病院　内科、帝京大学医学部附属病院　内科、東京医科大学八王子医療センター　消化器内科、東京慈恵会医科大学葛飾医療センター、東京都済生会中央病院　消化器内科、東邦大学医療センター大橋病院　消化器内科、東北大学病院　消化器内科、土佐市民病院　消化器内科、鳥取大学医学部　第2内科、富山大学附属病院　第三内科、富山県済生会富山病院　内科、長野県立木曽病院、那覇市立病院　内科、成羽病院　内科、南海病院　消化器内科、新潟臨港病院　内科、西脇市立西脇病院　消化器内科、白十字病院　肝臓内科、浜田医療センター　消化器内科、浜松医科大学　肝臓内科、東大和病院　消化器科、日高病院　内科、兵庫県立加古川医療センター　消化器内科、弘前大学　消化器内科、弘前市立病院、福岡赤十字病院　肝臓内科、福島県立医科大学　消化器・リウマチ・膠原病内科、防衛医科大学校　消化器内科、北部地区医師会病院　内科、北海道社会保険病院　消化器科、松下記念病院　消化器科、三菱神戸病院、武蔵村山病院　消化器内科、山形大学　消化器内科、山口大学　第一内科、山科病院　内科　（アイウエオ順）

G.研究発表

1．論文発表

Horie Y, Yamagishi Y, Ebinuma H, Hibi T. Obesity, Type 2 Diabetes, Age and Female Gender Are Significant Risk Factors in the Development of Alcoholic Liver Cirrhosis. Hepatol Int. 7: 280-285, 2013.

2．学会発表

平成25年度アルコール・薬物依存関連学会合同学術総会、第48回日本アルコール薬物医学会総会2013.10（岡山）

シンポジウム：アルコール性肝障害の新たな展開：新診断基準をふまえて　新診断基準を用いたアルコール性肝炎の診断と治療戦略

堀江義則、山岸由幸、海老沼浩利

第17回日本肝臓学会大会（東京）2013.10

中等症・重症アルコール性肝炎の予後についての検討

堀江義則、山岸由幸 、海老沼浩利、日比紀文

第40回日本肝臓学会西部会2013.12（岐阜市）

一般演題　栄養指導によるアルコール性肝障害の進展予防の提案

堀江義則、山岸由幸、海老沼浩利

H.　知的財産権の出願・登録状況

なし

表: 本邦における肝硬変の成因

	総数 (%)	男	女
HBV	810 (8.7%)	562 (9.7%)	248 (7.0%)
HBV+AL	167 (1.8%)	118 (2.0%)	49 (1.4%)
HCV	4046 (43.4%)	2120 (36.8%)	1926 (54.1%)
HCV+AL	353 (3.8%)	317 (5.5%)	36 (1.0%)
HBV+HCV	96 (1.0%)	63 (1.1%)	33 (0.9%)
HBV+HCV+AL	7 (0.1%)	5 (0.1%)	2 (0.1%)
AL	2293 (24.6%)	1979 (34.3%)	314 (8.8%)
その他	1517 (15.2%)	577 (10.0%)	940 (26.4%)
その他+AL	37 (0.4%)	27 (0.5%)	10 (0.3%)
合計	9326	5768	3558
うちアルコール性	2857 (30.6%)	2446 (42.4%)	411 (11.6%)

HBV：B 型肝炎、HCV：C 型肝炎、AL:アルコール性

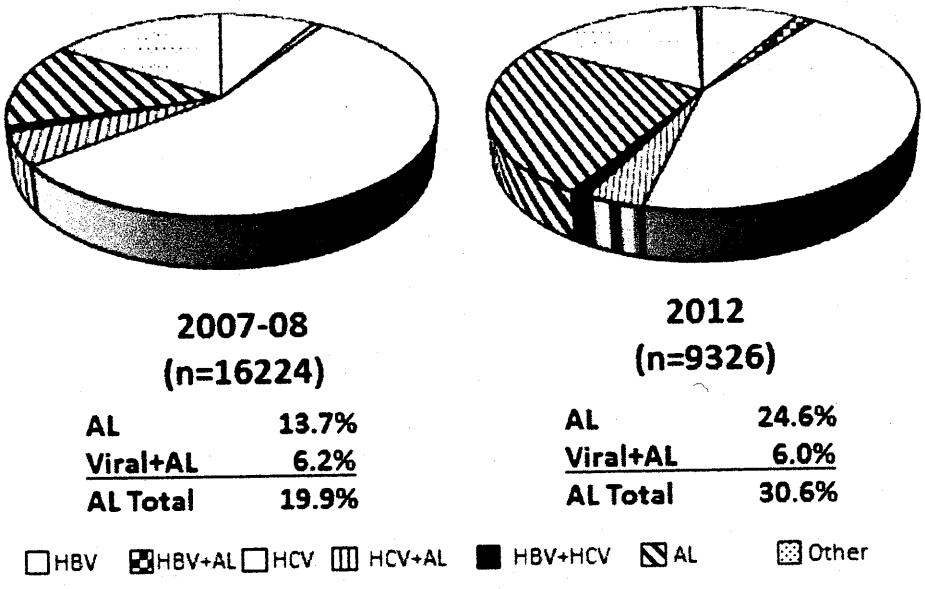

図：本邦における肝硬変の成因の推移

全肝硬変に占めるアルコール性の割合は、1997-1998 年度の 14%から 2012 年度は 25%（ウイルス性＋アルコール性を含めると 20%から 31%）に増加している。

HBV：B 型肝炎、HCV：C 型肝炎、AL:アルコール性

別紙4

雑誌

発表者氏名	論文タイトル名	発表誌名	巻号	ページ	出版年
Horie Y, Yamagishi Y, Ebinuma H, Hibi T.	Obesity, Type 2 Diabetes, Age and Female Gender Are Significant Risk Factors in the Development of Alcoholic Liver Cirrhosis.	Hepatol Int.	7	280-285	2013

Obesity, type 2 diabetes, age, and female gender: significant risk factors in the development of alcoholic liver cirrhosis

Yoshinori Horie, Yoshiyuki Yamagishi, Hirotoshi Ebinuma & Toshifumi Hibi

Hepatology International

ISSN 1936-0533
Volume 7
Number 1

Hepatol Int (2013) 7:280-285
DOI 10.1007/s12072-012-9347-6

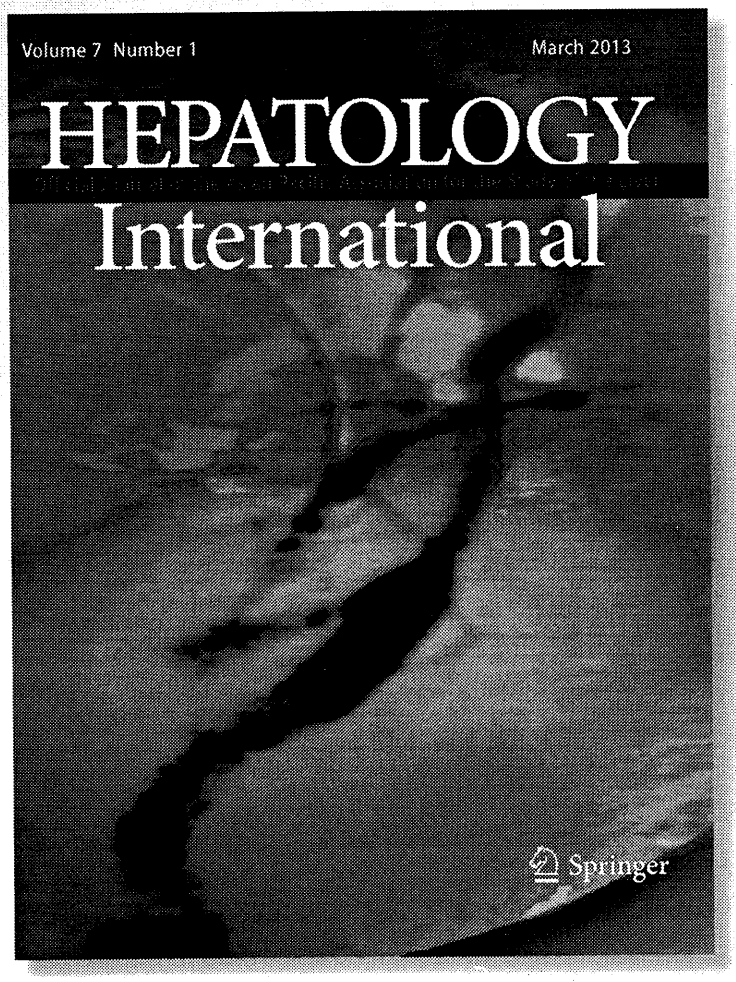

Springer